

Comparative study of Aluminum alloy, Gray CI, structural steel and Low alloy steel AISI 4140 spur gears using FEA and material testing

Jawahar Nishit Kumar¹, Gokula Krishnan Agilan², Sanjay Natarajan², Sundaramali Govindaswamy^{1*}

¹Department of Manufacturing Engineering, School of Mechanical Engineering (SMEC),

²Department of Electrical Engineering, School of Electrical Engineering (SELECT),
Vellore Institute of Technology, Vellore, Tamil Nadu, India – 632014

Abstract. Spur gears are commonly used for power transmission in mechanical systems. This research analyzes and compares spur gears made of four different materials - Aluminum alloy, Gray Cast Iron, Structural steel and low alloy steel AISI 4140. FEA was conducted to determine the effects of deformation, von Mises stress, and strain on the gearbox components, which indicated that they will perform adequately in relation to the loads associated with vehicle operation. This comparison evaluated the mechanical behavior within the operating conditions for gearbox components, such as von Miss stress and Von Miss strain. The FEA and mechanical testing demonstrated that these types of materials had comparable properties. The comparative analysis of mechanical properties of these materials and the design of the gearbox should be useful in helping to determine appropriate material selection for the manufacture of spur gears to be used in mechanical applications to transmit power.

1. Introduction

Spur gears represent some of the most common elements used in power transmission systems because of their simple construction, reliability, and compact size. Thus, spur gears are widely used in many industrial machinery and consumer products where power transmission must be reliable. Spur gears continue to be the predominant means of mechanical transmission in many systems because of their high efficiency and compact size [1]. Numerical methodologies (most notably Finite Element Analysis (FEA)) have been used extensively to investigate the structural performance of spur gears. Static structural analysis provides insight into the distribution of stresses, deformations, and safety factors as they relate to various operational conditions.

* Corresponding author: sundaramali.g@vit.ac.in

One research group used ANSYS 15.0 and combined its capabilities with various decision support methods (COPRAS and MOORA) to evaluate the structural qualities of materials historically used in manufacturing spur gear, including structural steel, AlSiC (Aluminum Silicon carbide composite), AISI alloy steel, and Titanium Ti6242S. The group found equivalent structural performance characteristics between structural steel, AlSiC, and AISI 4140, while the group identified titanium Ti6242S as the preferred material to manufacture spur gears using both COPRAS and TOPSIS decision-making methodologies [2]. Research teams have also proposed advanced materials selection methodologies that utilize Ashby's charts to design high strength and lightweight spur gears. Through clearly defining objective functions, constraints, and performance indices, research teams have evaluated multiple materials' criteria relating to strength, weight, and fatigue resistance. Using bending fatigue as the primary failure mode criterion, both titanium and beryllium base alloys produced substantially reduced weights of spur gears compared to conventional materials. [3]. Research has been performed into the fatigue damage of spur gears, specifically through experimental means with AISI 4140 gear material. The results of single tooth bending fatigue tests conducted have shown that increased surface hardness results in greater residual stresses being present therefore shortening the overall life of the gear under those conditions. The initiation and propagation of cracks were found to occur primarily at the tooth root for the symmetrical spur gear [4].

The results of experiments that were conducted to determine the overall efficiency of spur gears under varying speed and load conditions showed that the module of the spur gear had the largest effect on the overall efficiency of spur gears; while the surface roughness had a lesser affect than the spur gear module. The most influential factor about loss of power associated with spur gears was determined to be the viscosity of the lubricant being used; however, lower viscosity lubricants were shown to improve the overall efficiency of spur gears only under specific operating conditions [5]. The vibration-based diagnostic techniques described herein were employed to evaluate wear and lubrication-related failure modes of spur gears in this study. The Morlet wavelet transform analysis technique was used to measure gear faults caused by lubrication failure; the analysis demonstrated that lubrication failure contributed significantly to the gear faults. In addition, the associated changes in the amplitude of the wavelet energy corresponded well to the degree of gear tooth damage, which will assist in the early identification of failure modes and condition monitoring of spur gears [6]. Micro-pitting and scouring failure modes were found to correlate with reductions in the stiffness of the spur gears and as such, increase the vibration levels. Modal analysis techniques were demonstrated to be useful in the identification of reality of stiffness reductions due to wear, while the hardness of the spur gear was found to affect the pitting resistance. [7]. The comparison of the structural properties of composite spur gears made from materials such as carbon epoxy and their metal counterparts show that while composite spur gears have lower stress levels than cast steel spur gears, many composites have greater deformation than cast steels. In addition, it was found that composite spur gears exhibit less weight than their metallic counterparts[8].

Fatigue-induced tooth root fracture was found to be the predominant failure mode in electric vehicle (EV) transmission gears based on the results of the failure analysis. The combination of the results of the experimental and FEA tests showed that high contact stress, impact loading, and insufficient alloying contributed to intergranular brittle fracture of the transmission gears, leading to premature failure. [9].

The spur gears were designed based on standard gearbox specifications and modeled in Fusion 360. FEA was used for stress, strain, and deformation analysis at the gear tooth for a given load condition while using four separate materials to compare; Aluminum Alloy NL, Gray Cast Iron, Structural Steel, and low Alloy Steel AISI 4140. The results from the simulation found that Aluminum Alloy NL and Gray Cast Iron had higher deformation and stress levels which make these materials unsuitable for high load applications. The structural steel and AISI 4140 samples had a superior mechanical performance than the other two materials, as the FEA results indicated lower levels of stress concentration and greater levels of stiffness. Therefore, the focus of comparative analysis moved to structural steel versus AISI 4140. To ensure the validity of the numerical analysis, several tests were performed on both materials; hardness, tensile strength, chemical composition, and wear testing. AISI 4140 had greater strength and superior wear resistance compared to structural steel; therefore, AISI 4140 has an advantage for durability under continuous operation, as reduced wear reduces material loss and improves mechanical efficiency. Based on the analytical and experimental results, a prototype spur gear gearbox was built. This system consists of an input shaft and an output shaft that connect with an input crank and output crank respectively. A prototype that works at 500 rpm was built to investigate if the chosen material could be used practically. The goal of this study is to determine whether low Alloy Steel AISI 4140 could be used as an alternate material for constructing spur gears instead of using Structural Steel. This research will determine the impact of selecting either type of material on how gears experience stress during operation, how well they resist wear and how mechanically efficient they are. Improving gear performance and their service life can help develop better power transmission systems.

2.Methodology

2.1 Research Execution Stages

A systematic approach (multi-step design method) developed for meeting the research objectives. Initially, reviewed literature related to spur gear FEA and additional material selections. At the same time, a spur gear designed according to industry standards was also analyzed. Following that, two spur gears and one constant mesh (spindle arrangement) were produced and analyzed using FEA techniques as well. These analyses were conducted under various constraints and boundary conditions using different materials. Based on the analyzed results, the materials were selected for further lab study. Finally, using the insights gained from these tests, a prototype model of a gearbox was fabricated as the culmination of the study.

2.2 Selection of materials

The primary sorting of materials was done using the literature study, current materials used in a gearbox of a vehicle, and the Ashby chart. The Ashby Material Selection Method is utilized to rank spur gear manufacturing materials by quantitative ranking. The design criterion calls for a material that provides a combination of high stiffness and strength, with the minimum amount of weight, while also providing resistance to bending failure at the root area of the gear tooth.

The relationship between the materials' elastic modulus and yield strength of the materials used to manufacture the spur gear tooth is that the amount of bending stress is inversely

proportional. Therefore, to reduce the amount of weight of the spur gear tooth, the density of the materials must be less than required. As a result, the performance index for a spur gear tooth that is light and stiff can be described as follows.:

$$M_1 = \rho/E$$

where **E** is Young’s modulus and **ρ** is density. A higher value of M_1 indicates a better stiffness-to-weight ratio.

Similarly, to maximize strength while minimizing weight, the strength-based performance index can be expressed as:

$$M_2 = \sigma_y / \rho$$

where **σ_y** is yield strength and **ρ** is density. A higher value of M_2 indicates a better strength-to-weight ratio.

Using the mechanical properties from Table 1, the performance indices M_1 and M_2 were calculated for each material. Table 1 presents the ranking based on Ashby performance indices.

Table 1: Ashby Index Calculation Table.

Material	Density (Kg/m ³)	Young’s Modulus E (GPa)	Yield Strength σ _y (MPa)	$M_1 = \rho/E$ (×10 ⁶)	$M_2 = \sigma_y / \rho$ (×10 ⁶)
Aluminum Alloy	2770	71	280	25.63	101.08
Gray Cast Iron	7150	110	200	15.38	27.97
Structural Steel	7900	200	250	25.32	31.65
AISI 4140	7850	200	415	25.48	52.87

Based on this study it was identified structural steel is being used in vehicles, Gray Cast iron has been analyzed to compare various other materials, Aluminum alloy which is used for the comparative study and a material selected using the Ashby chart namely AISI 4140 low alloy steel which is lightweight and economically feasible compared to other lightweight alloys.

2.3 CAD Modelling of spur gear:

The spur gear pair was modelled using fusion 360, and gear dimensions are listed in the table below. The dimensions were specifically similar to spur gears used in the gearboxes of 4-wheeled vehicles to keep the study closer to the real case scenario. Primary analysis is with single spur gear analyzed under various conditions for selected materials. Secondary analysis is with the gear pair of an automobile 4-wheeler vehicle gearbox that has been modelled and analyzed using analysis software under various boundary conditions and constraints. Based on these results, a constant mesh gear train is analyzed under similar conditions and constraints. These analyses are completed using FEA software Ansys. Table 2 shows the spur gear dimensions.

The applied torque values (132 N·m, 2300 N·m, and 10278 N·m) were selected to represent low-load, nominal-load, and extreme overload conditions encountered in automotive gearbox

applications. These values allow evaluation of the gear structural response across realistic service torque and peak loading cases.

Table 2: Spur Gear Dimensions Primary gear and secondary gear

Parameters	Primary gear	Secondary gear
Module (M)	2.50 mm	2.60 mm
Pitch Circle Diameter (D)	90 mm	26 mm
Nos. of Teeth (z)	36	10
Thickness of tooth (t)	15.7 mm	15.7 mm
Pressure angle (ϕ)	20	20

2.4. Static Structural Analysis of Gears

Gears are analyzed statically for their structural integrity. Static structural analysis of gears is an analytical procedure to investigate gear tooth behavior under static loads (or slowly changing loads). Static structural analyses primarily focus on evaluating how gears distribute stress, deform, react to contact pressures, and ensure they have sufficient safety factors to operate without failure. Static structural analysis of gears evaluates tooth bending and contact stresses to determine if the gear will be able to withstand the applied torque. Static structural analysis is referred to as static because it does not account for dynamic loads induced by vibration, inertia, or high-speed impacts during normal operation of the gears in service.

2.4.1 Aluminum alloy

In Figure 1, the outcomes of static structural analysis of Aluminum alloy NL at 132 N-m. The parameters observed are total deformation, von Mises stress, and von Mises strain. Notable observations reveal a maximum deformation of 0.021 mm and a minimum deformation of 0.002 around the contact region. The maximum von Mises stress and strain are 115.93 MPa and 0.0016 mm/mm.

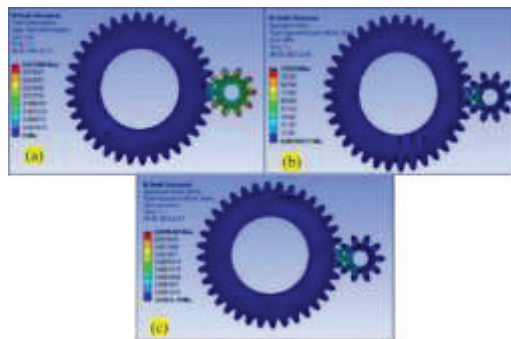


Fig 1. Static structural analysis of Aluminum alloy NL at 132 N-m (a) Total Deformation (b) Von mises stress (c) Von mises strain

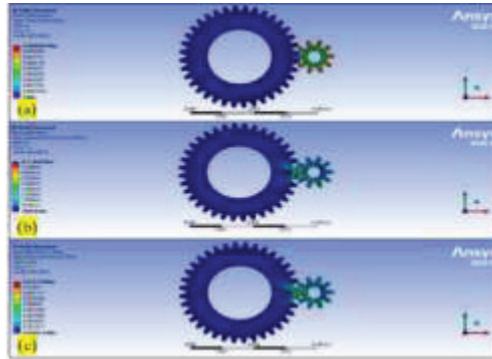


Fig 2. Static structural analysis of Aluminum alloy NL at 2300 N-m **(a)** Total deformation **(b)** Von Mises stress **(c)** Von Mises strain

In Figure 2, the outcomes of the static structural analysis of Aluminum alloy NL at 2300 N-m. The parameters observed are total deformation, von Mises stress, and von Mises strain. Notable observations reveal a maximum deformation of 6.6 mm and a minimum deformation of 0.007 around the contact region. The maximum von mises stress and strain are 811.6 MPa and 0.0117 mm/mm.

In Figure 3, the outcomes of static structural analysis of Aluminum alloy NL at 10278 N-m. The parameters observed are total deformation, von Mises stress, and von Mises strain. Notable observations reveal a maximum deformation of 9.6 mm and a minimum deformation of 1.2 mm around the contact region. The maximum von Mises stress and strain are 420 MPa and 0.0058 m/m.

In Figure 4, the results of static structural analysis of Low alloy NL at 132 N-m. The parameters observed are total deformation, Von mises stress, and von Mises strain. Notable observations reveal a maximum deformation of 0.00729 mm and a minimum deformation of 0.0008 around the contact region. The maximum von Mises stress and strain are 115.55 MPa and 0.000548 mm/mm.

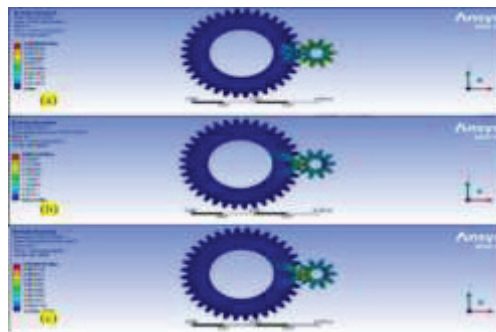


Fig 3. Static structural analysis of Aluminum alloy NL at 10278 N-m **(a)** Total Deformation **(b)** Von Mises stress **(c)** Von Mises strain

2.4.2 Static Structural Analysis of AISI 4140

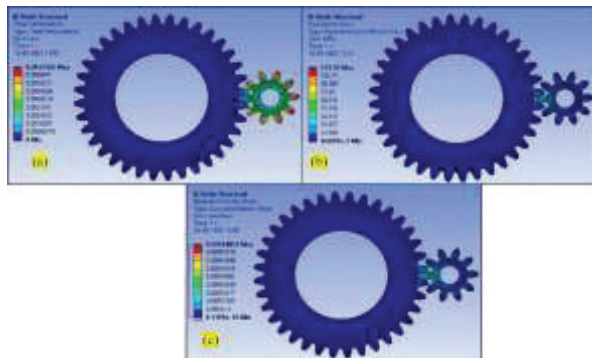


Fig 4. Static structural analysis of Low alloy steel AISI 4140 at 132 N-m (a) Total deformation (b) Von Mises stress (c) Von Mises strain

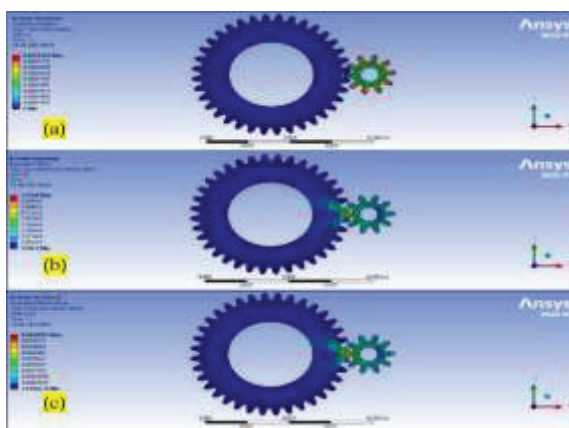


Fig 5. Static structural analysis of Low alloy steel AISI 4140 at 2300 N-m (a) Total deformation (b) Von Mises stress (c) Von Mises strain

In Figure 5, the outcomes of the results of static structural analysis of Low alloy steel at 2300 N-m. The parameters observed are total deformation, von Mises stress, and von Mises strain. Notable observations reveal a maximum deformation of 0.001 mm and a minimum deformation of 0.0001 mm around the contact region. The maximum von Mises stress and strain are 707 MPa and 0.0034 mm/mm.

In Figure 6, the outcomes of the results of static structural analysis of Low alloy steel AISI 4140 at 10278 N-m. The parameters observed are total deformation, von Mises stress, and von Mises strain.

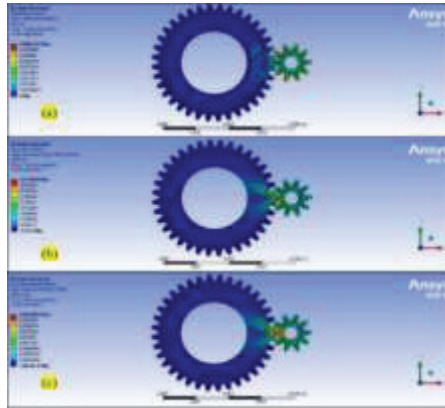


Fig 6. Static structural analysis of Low alloy steel AISI 4140 at 10278 N-m **(a)** Total Deformation **(b)** Von Mises stress **(c)** Von Mises strain

Notable observations reveal a maximum deformation of 0.006 mm and a minimum deformation of 0.0007 mm around the contact region. The maximum von Mises stress and strain are 563 MPa and 0.002 mm/mm.

2.4.3 Static Structural analysis of gray cast iron

In Figure 7, the outcomes of the results of static structural analysis of Gray Cast Iron at 132 N-m. The parameters observed are total deformation, von Mises stress, and von Mises strain. Notable observations reveal a maximum deformation of 0.015 mm and a minimum deformation of 0.0016 mm around the contact region. The maximum von Mises stress and strain are 117.09 MPa and 0.001 mm/mm.



Fig 7. Static structural analysis of Gray Cast Iron at 132 N-m **(a)** Total Deformation **(b)** Von Mises stress **(c)** Von Mises strain

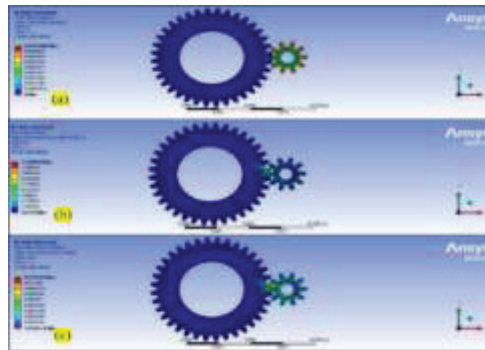


Fig 8. Static structural analysis of Gray Cast Iron at 2300 N-m (a) Total deformation (b) Von Mises stress (c) Von Mises strain

In Figure 8, the outcomes of the results of static structural analysis of Gray Cast Iron at 2300 N-m. The parameters observed are total deformation, von Mises stress, and von Mises strain. Notable observations reveal a maximum deformation of 0.5 mm and a minimum deformation of 0.05 mm around the contact region. The maximum von Mises stress and strain are 1130 MPa and 0.012 mm/mm.

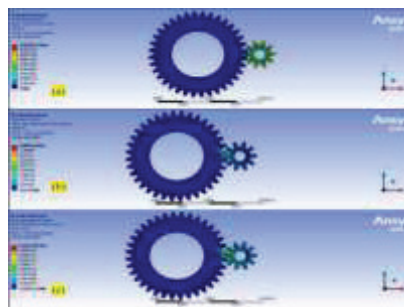


Fig 9. Static structural analysis of Gray Cast Iron at 10278 N-m (a) Total deformation (b) Von Mises stress (c) Von Mises strain

In Figure 9, the outcomes of the results of static structural analysis of Gray Cast Iron at 10278 N-m. The parameters observed are total deformation, von Mises stress, and von Mises strain. Notable observations reveal a maximum deformation of 3.29 mm and a minimum deformation of 0.3 mm around the contact region. The maximum von Mises stress and strain are 868 MPa and 0.008 mm/mm.

2.4.4 Static Structural Analysis of Structural steel

In Figure 10, the outcomes of the results of static structural analysis of Structural Steel at 132 N-m. The parameters observed are total deformation, von Mises stress, and von Mises strain. Notable observations reveal a maximum deformation of 0.005 mm and a minimum deformation of 0.0005 mm around the contact region. The maximum von Mises stress and strain are 1400 MPa and 0.011 mm/mm.



Fig 10. Static structural analysis of Structural steel at 132 N-m (a) Total Deformation (b) Von Mises Stress (c) Von Mises Strain

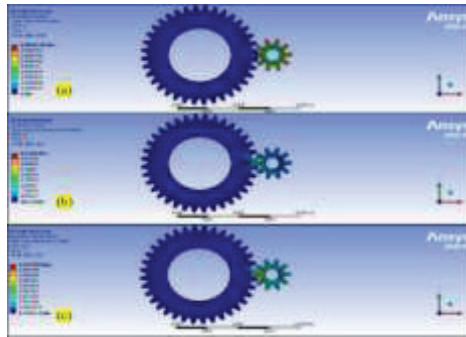


Fig 11. Static structural analysis of Structural steel at 2300 N-m (a) Total Deformation (b) Von Mises stress (c) Von Mises strain

In Figure 11, the outcomes of the results of static structural analysis of Structural Steel at 2300 N-m. The parameters observed are total deformation, von Mises stress, and von Mises strain. Notable observations reveal a maximum deformation of 0.0009 mm and a minimum deformation of 0.0001 mm around the contact region. The maximum von Mises stress and strain are 623 MPa and 0.005 mm/mm.

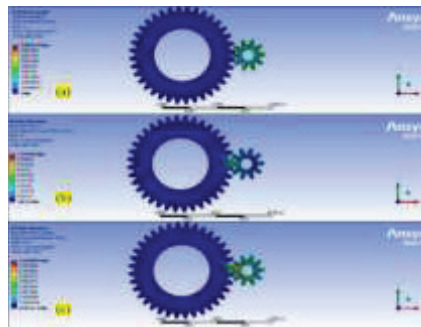


Fig 12. Static structural analysis of Structural steel at 10278 N-m (a) Total Deformation (b) Von Mises stress (c) Von Mises strain

In Figure 12, the outcomes of the results of static structural analysis of Structural Steel at 10278 N-m. The parameters observed are total deformation, von Mises stress, and von Mises strain. Notable observations reveal a maximum deformation of 0.004 mm and a minimum deformation of 0.00044 mm around the contact region. The maximum von Mises stress and strain are 727 MPa and 0.0044 mm/mm.

2.5 Explicit Dynamics

A frictional contact formulation was applied between meshing gear tooth surfaces with a coefficient of friction $\mu = 0.15$. The bore/inner faces of the gears were constrained to represent shaft support using fixed support boundary conditions. Automatic stable time stepping was used in the explicit solver, with the time step controlled by the Courant stability criterion.

Explicit dynamics is a method used when conditions applied to the model are under continuous change. It is a time integration method which is specifically used when the speed applied to the model has a major effect on the component and in designing the same. Here, friction bonding was given under contact. Both inner faces were under fixed support constraints. An angular velocity of 1000 rads/s was applied to the secondary gear. As the spur gears are under constant rotational motion, the above-mentioned constraints have been applied on the body. The results obtained might be satisfactory.

2.5.1 Explicit Dynamics analysis of Aluminum alloy

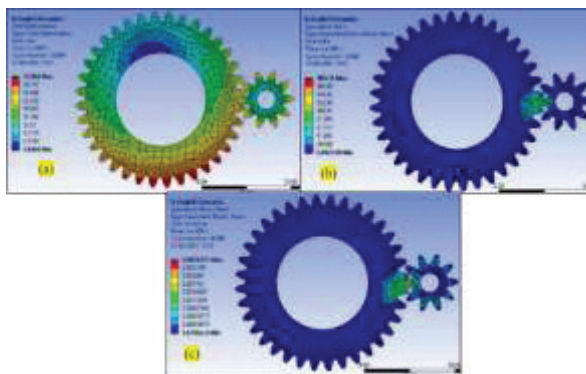


Fig 13. Explicit dynamics of Aluminum alloy NL (a) Total Deformation (b) Von Mises stress (c) Von Mises strain

Observing Table 3 the outcomes of 10278 N-m the total deformation of aluminum alloy NL is 0.0096066 mm and possesses a von Mises Stress of 400 MPa and a strain of 0.0058 mm/mm. From Figure 13 notable observations reveal the changes in the gear's mesh after 32369 cycles and visualize what the data is reporting. The observations were recorded at 132, 2300, and 10278 N-m to compare the difference in the same parameters across the different materials, in the same test conditions.

2.5.2 Explicit Dynamics analysis of AISI 4140

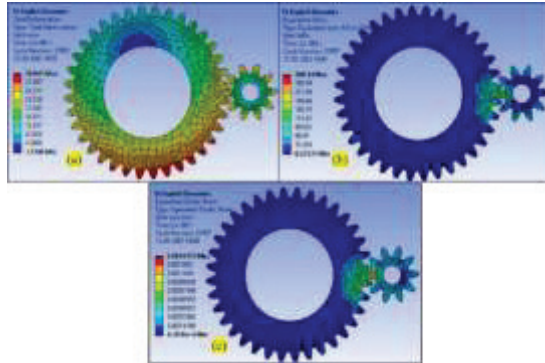


Fig 14. Explicit dynamics of Low alloy steel AISI 4140 (a) Total Deformation (b) Von Mises Stress (c) Von Mises strain

Observing Table 3 the outcomes of 10278 N-m the total deformation of Low Alloy Steel is 0.0063052 mm and possesses a von Mises Stress of 565 MPa and a strain of 0.0026 mm/mm. From Figure 14 notable observations reveal observe the changes in the gear’s mesh after 31957 cycles and visualize what the data is reporting. At 10278 N-m the Low alloy steel AISI 4140 has a lesser total deformation and higher von Mises stress than Aluminum Alloy NL, the difference in von Mises strain is negligible.

2.5.3 Explicit Dynamics analysis of gray cast iron

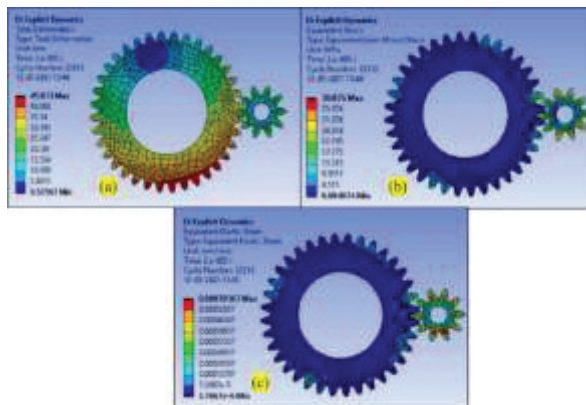


Fig 15. Explicit dynamics of Gray Cast Iron (a) Total Deformation (b) Von Mises stresses (c) Von Mises strain

Observing Table 3 the outcomes of 10278 N-m the total deformation of Gray Cast Iron is 0.0032 mm which is lesser than the previous two materials and possesses a von Mises Stress of 880 MPa and a strain of 0.0812 mm/mm both of which are considerably higher than the previous two materials. From Figure 15 notable observations reveal that they can observe the changes in the gear mesh after 23212 cycles and visualize what the data is reporting. The data suggests that using Gray Cast Iron would make the gear more susceptible to failing as compared to the other materials.

2.5.4 Explicit Dynamics analysis of structural steel

Observing Table 3 the outcomes of see that at 10278 N-m the total deformation of structural steel is 0.004034 mm and possesses a von Mises Stress of 720 MPa and a strain of 0.0044 mm/mm. From Figure 16 notable observations reveal the changes in the gear’s mesh after 30741 cycles and visualize what the data is reporting. From the data, structural steel performs better than most materials in terms of deformation; however, it possesses a significantly high von Mises Stress as compared to the other materials.

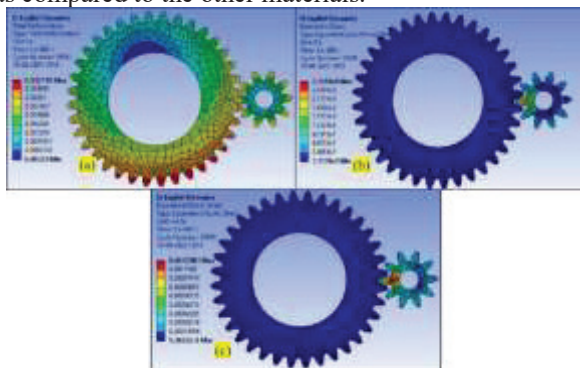


Fig 16. Explicit Dynamics of structural steel (a)Total Deformation (b) Von Mises stresses (c) Von Mises strain

2.6 Data Analysis

2.6.1 Finite Element Analysis Data

Table 3: Static structural analysis result data table

Failure theories	Load	Total deformation (mm)	Von Mises stress (MPa)	Von Mises strain(mm)
Aluminum Alloy NL	132 N-m	0.021668	115.93	0.0016465
	2300 N-m	0.006672	811.16	0.0011714
	10278 N-m	0.0096066	400.27	0.0058648
Gray Cast Iron	132 N-m	0.015063	117.09	0.001065
	2300 N-m	0.52688	1399.8	0.0012784
	10278 N-m	0.003291	888.82	0.08128
Structural steel	132 N-m	0.00092196	116.234	0.005392
	2300 N-m	0.005179	144.6	0.01105
	10278 N-m	0.004034	727.49	0.0044591
Low alloy steel AISI 4140	132 N-m	0.0072429	115.55	0.00054831
	2300 N-m	0.0010325	707	0.00340597
	10278 N-m	0.0063052	565.38	0.002689

Comparing all four materials under three different moments and similar constraints, it showed us that the values calculated were almost similar in all cases. The spur gear pairs have almost the same values, but AISI 4140 low alloy steel has shown less deformation when compared to the other two materials. Von Mises stress is negligible for all the materials.

2.6.2 Explicit Dynamics Data

Table 4: Total deformation Explicit Dynamics data of Aluminum Alloy NL

Time [s]	Minimum [mm]	Maximum [mm]	Average [mm]
1.1755*10 ³⁸	0	3.5804*10 ⁻¹⁵	9.4165*10 ⁻¹⁷
0.0001003	6.1437*10 ⁻²	1.5838	0.35062
0.0002001	0.39548	3.1497	1.5645
0.0003002	0.73805	4.7069	2.844
0.0004003	1.0522	6.2635	4.0868
0.0005005	1.3393	8.2032	5.2934
0.0006001	1.601	10.092	6.4636
0.0007004	1.839	11.933	7.5996
0.0008001	2.0545	13.725	8.7005
0.0009005	2.2493	15.471	9.7684
0.001	2.4244	17.171	10.802
0.0011	2.5816	18.826	11.804
0.0012	2.6917	20.438	12.774
0.0013001	2.7769	22.009	13.713
0.0014	2.841	23.538	14.62
0.0015	2.8849	25.028	15.498
0.0016	2.9098	26.479	16.346
0.0017	2.9168	27.903	17.165
0.0018	2.9068	29.292	17.956
0.0019	2.881	30.647	18.719
0.002	2.8404	31.969	19.455

Table 5: Total deformation Explicit dynamics data of Low alloy steel AISI 4140

Time [s]	Minimum [mm]	Maximum [mm]	Average [mm]
1.1755*10 ⁻³⁸	0.0	3.5804*10 ⁻¹⁵	9.4165*10 ⁻¹⁷
0.0001004	3.6993*10 ⁻²	1.5891	0.29114
0.0002001	0.24152	3.1757	1.2848
0.0003001	0.50055	4.7353	2.4901
0.0004006	0.75115	6.2866	3.6868
0.0005001	0.97613	7.8225	4.8484
0.0006003	1.1774	9.3657	5.9776
0.0007006	1.3565	11.161	7.0742
0.0008003	1.5149	12.91	8.1381
0.0009	1.6544	14.616	9.1705

0.001	1.7765	16.28	10.173
0.0011	1.883	17.902	11.144
0.0012	1.9755	19.484	12.085
0.0013001	2.0139	21.026	12.998
0.0014	2.028	22.53	13.881
0.0015	2.0225	23.997	14.736
0.0016	1.9983	25.428	15.563
0.0017	1.9563	26.824	16.364
0.0018	1.8977	28.192	17.137
0.0019	1.8234	29.532	17.885

Table 6: Total deformation Explicit dynamics data of Gray Cast Iron

Time [s]	Minimum [mm]	Maximum [mm]	Average [mm]
1.1755*10 ⁻³⁸	0.0	3.5804*10 ⁻¹⁸	9.4165*10 ⁻¹⁷
0.0001004	9.5341*10 ⁻²	1.5811	0.41363
0.0002001	0.72897	3.414	2.2583
0.0003001	1.3259	6.5462	4.1502
0.0004006	1.2857	9.2101	5.6049
0.0005001	1.0271	11.708	6.9241
0.0006003	0.76771	14.171	8.2328
0.0007006	0.55267	16.596	9.5251
0.0008003	0.50472	18.983	10.8
0.0009	0.70127	21.333	12.056
0.001	0.81794	23.647	13.293
0.0011	0.57754	25.926	14.511
0.0012	0.38449	28.167	15.709
0.0013001	0.40036	30.376	16.888
0.0014	0.64943	32.558	18.046
0.0015	0.62377	34.716	19.185
0.0016	0.48496	36.841	20.305
0.0017	0.57063	38.935	21.407
0.0018	0.84501	40.997	22.49
0.0019	0.75804	43.03	23.554
0.002	0.51507	45.033	24.601

Table7: Total deformation Explicit dynamics data of structural steel

Time [s]	Minimum [m]	Maximum [m]	Average [m]
1.1755*10 ⁻³⁸	0.0	3.5804*10 ⁻¹⁸	9.4165*10 ⁻²⁰
0.0001006	0.00066023	0.0017789	0.0003662
0.0002003	0.0041026	0.0032345	0.001599
0.0003001	0.0077098	0.004791	0.0029018
0.0004002	0.0011041	0.0064019	0.0041690
0.0005005	0.001411	0.00803419	0.0054008
0.0006002	0.0016296	0.010309	0.0065968
0.0007001	0.0019516	0.012190	0.0077584
0.0008003	0.0021183	0.0140230	0.00886
0.0009	0.0024046	0.015810	0.099801
0.001	0.0026071	0.017552	0.011041
0.0011	0.0027734	0.019250	0.012070
0.0012	0.0029031	0.020905	0.013067
0.0013001	0.0030086	0.022516	0.014033
0.0014	0.0030994	0.024089	0.014967
0.0015	0.0031604	0.025620	0.015872
0.0016	0.0032076	0.027170	0.016747
0.0017	0.0032371	0.028586	0.017592
0.0018	0.0032371	0.030017	0.018408
0.0019	0.00325	0.031413	0.019197
0.002	0.00323	0.031413	0.019957

Comparing the explicit dynamics results (Table 4-7) which show us the deformation of the gears during instant velocity changes, states that Low alloy steel AISI 4140 has lesser value of total deformation when compared to the other two materials.

4. Conclusion

The Spur gear pair was designed in fusion 360 with dimensions like gears used in vehicles. They were imported into analysis software for static structural analysis under similar conditions for all materials.

- From static structural analysis data, it is seen that gray cast iron and Aluminum alloy have similar results, AISI 4140 material and Structural steel has shown very similar deformation on the tooth.
- Even though the deformation looks similar, the values vary under different moments and speed. With the obtained values gray cast iron and Aluminum alloy have more deformation.
- AISI 4140 and structural steel have shown similar results in static structural analysis with almost the same values.
- Dynamic explicit analysis also has the same conditions where AISI 4140 and structural steel have shown better results under various constraints and conditions.

The author(s) declare that no external financial support for the research, authorship, and/or publication of this article was received for this study. Data will be made available on request.

References

- [1]. T. Praveenkumar, M. Saimurugan, and K. I. Ramachandran, “Comparison of Vibration, Sound and Motor Current Signature Analysis for Detection of Gear Box Faults,” *Int J Progn Health Manag*, vol. 8, no. 2, Nov. 2020, doi: 10.36001/ijphm.2017.v8i2.2642.
- [2]. A. C. Ram Kumar, N. Mohammed Raffic, K. Ganesh Babu, and S. Selvakumar, “Static structural analysis of spur gear using ANSYS 15.0 and material selection by COPRAS, MOORA techniques,” *Materials Today Proceeding*, vol. 47, pp. 25–36, 2021, doi: 10.1016/j.matpr.2021.03.485.
- [3]. H. Delibaş, Ç. Uzay, and N. Geren, “Advanced Material Selection Technique For High Strength and Lightweight Spur Gear Design,” *European Mechanical Science*, vol. 1, no. 4, pp. 133–140, Dec. 2017, doi: 10.26701/ems.352444.
- [4]. S. Mehmet Demet and A. Serhat Ersoyoglu, “Investigation of the effect of hardness on gear tooth failure by bending fatigue test,” *Selcuk University Journal of Engineering Sciences*, vol. 21, no. 03, pp. 127–130, 2022, [Online]. Available: <http://sujes.selcuk.edu.tr>
- [5]. T. T. Petry-Johnson, A. Kahraman, N. E. Anderson, and D. R. Chase, “An Experimental Investigation of Spur Gear Efficiency,” *Journal of Mechanical Design*, vol. 130, no. 6, Jun. 2008, doi: 10.1115/1.2898876.
- [6.] M. Amarnath and C. Sujatha, “Surface Contact Fatigue Failure Assessment in Spur Gears Using Lubricant Film Thickness and Vibration Signal Analysis,” *Tribology Transactions*, vol. 58, no. 2, pp. 327–336, Mar. 2015, doi: 10.1080/10402004.2014.971993.
- [7]. M. Amarnath, S. Chandramohan, and S. Seetharaman, “Experimental investigations of surface wear assessment of spur gear teeth,” *Journal of Vibration and Control*, vol. 18, no. 7, pp. 1009–1024, 2012, doi: 10.1177/1077546311399947.
- [8]. V. R. Gajender and T. Jeyapooan, “Design and Stress Strain Analysis of Composite Spur Gear in Automobile,” *International Journal of Engineering Sciences*, (Vol. 5, Number 5, pp. 144–156), 2016, doi: 10.5281/zenodo.51011.
- [9]. W. Feng, Z. Feng, and L. Mao, “Failure analysis of a secondary driving helical gear in transmission of electric vehicle,” *Eng Fail Anal*, vol. 117, p. 104934, Nov. 2020, doi: 10.1016/j.engfailanal.2020.104934.